



# CTRPI3 Protects H9c2 Cells Against Hypoxia/Reoxygenation (H/R)-Induced Injury Via Regulating the AMPK/Nrf2/ARE Signaling Pathway

Cell Transplantation  
Volume 30: 1–13  
© The Author(s) 2021  
Article reuse guidelines:  
sagepub.com/journals-permissions  
DOI: 10.1177/09636897211033275  
journals.sagepub.com/home/ccl  


Weifeng Jiang<sup>1</sup> , Jungang Song<sup>1</sup>, Suitao Zhang<sup>1</sup>, Yanyan Ye<sup>1</sup>, Jun Wang<sup>2</sup>, and Yilin Zhang<sup>1</sup>

## Abstract

Myocardial infarction (MI) is identified as the myocardial necrosis due to myocardial ischemia/reperfusion (I/R) injury and remains a leading cause of mortality. C1q/TNF-related protein 13 (CTRPI3) is a member of CTRP family that has been found to be involved in coronary artery disease (CAD). However, the role of CTRPI3 in MI remains unclear. We aimed to explore the functional role of CTRPI3 in H9c2 cells exposed to hypoxia/reoxygenation (H/R). Our results demonstrated that H/R stimulation significantly decreased the expression of CTRPI3 in H9c2 cells. H/R-induced an increase in ROS production and reductions in activities of SOD and CAT were prevented by CTRPI3 overexpression but were aggravated by CTRPI3 silencing. Moreover, CTRPI3 overexpression could reverse the inductive effect of H/R on caspase-3 activity and bax expression, as well as the inhibitory effect of H/R on bcl-2 expression in H9c2 cells. However, CTRPI3 silencing presented opposite effects with CTRPI3 overexpression. Furthermore, CTRPI3 overexpression enhanced the H/R-stimulated the expression levels of p-AMPK and nuclear Nrf2, and Nrf2 transcriptional activity. However, inhibition of AMPK reversed the CTRPI3-mediated activation of Nrf2/ARE signaling and the cardiac-protective effect in H/R-exposed H9c2 cells. Additionally, silencing of Nrf2 reversed the protective effects of CTRPI3 against H/R-stimulated oxidative stress and apoptosis in H9c2 cells. Finally, recombinant CTRPI3 protein attenuated myocardial I/R-induced injury in rats. Taken together, these findings indicated that CTRPI3 protected H9c2 cells from H/R-stimulated oxidative stress and apoptosis via regulating the AMPK/Nrf2/ARE signaling pathway. Our results provided evidence for the therapeutic potential of CTRPI3 in myocardial I/R injury.

## Keywords

myocardial infarction (mi), myocardial ischemia/reperfusion (i/r) injury, c1q/TNF-related protein 13 (ctrp13), oxidative stress; apoptosis, ampk/nrf2/are signaling pathway,

## Introduction

Myocardial infarction (MI) is a term for an event of heart attack with the symptoms of chest pain, shortness of breath, abnormal heart beating, sweating, nausea, vomiting, anxiety, and fatigue<sup>1</sup>. The understanding of the pathogenesis of MI has evolved over the past decades and new treatment strategies have greatly improved survival. Nevertheless, patients who develop cardiogenic shock still face challenges with a high 30-day mortality of at least 40%<sup>2</sup>.

The occurrence of MI is due to formation of plaques in the interior walls of the arteries resulting in reduced blood flow to the heart and heart injury because of lack of oxygen supply<sup>3</sup>. Appropriate reperfusion therapy has been demonstrated to reduce long-term complications of infarction, including

mortality, by as much as 50% to 70%<sup>4</sup>. However, the restoration of blood flow is known to induce a burst of reactive oxygen species (ROS) production and oxidative damage, which leads to a greater myocardial tissue injury than that

<sup>1</sup> Department of Cardiology, Kaifeng People's Hospital, Kaifeng 475000, China

<sup>2</sup> Teaching and Research Office of Human Anatomy, School of Basic Medical Sciences, Henan University, Kaifeng 475004, China

Submitted: July 10, 2020. Revised: April 27, 2021. Accepted: June 30, 2021.

### Corresponding Author:

Weifeng Jiang, Department of Cardiology, Kaifeng People's Hospital, Kaifeng 475000, China.  
Email: jangweifeng@126.com



caused by the original ischemic insult<sup>5</sup>. Thus, prevention of the oxidative damage is one of the effective ways of protecting the heart from myocardial ischemia/reperfusion (I/R) injury.

The C1q/TNF-related protein (CTRP) family of proteins is rapidly growing and currently comprises a further 15 members in addition to adiponectin<sup>6</sup>. CTRP proteins have attracted much interest due to the specific structure composed of four distinct domains: a signal peptide at the N terminus, a short variable region, a collagenous domain, and a C-terminal globular domain that is homologous to complement component 1q (C1q)<sup>6</sup>. To date, 15 additional CTRP family members have been identified to play roles in various biological processes, such as metabolism and immunity<sup>7</sup>.

CTRP13 is a secreted adipokine that plays important roles in several cardiovascular diseases. For instance, CTRP13 is involved in the development and prognosis of coronary artery disease (CAD) by modulating metabolic pathways, influencing immuno-inflammatory response and regulating cardiovascular functions<sup>8</sup>. CTRP13 inhibits atherosclerosis through preventing atherosclerotic plaque formation via modulation of lipid uptake and foam-cell migration<sup>9</sup>. However, the role of CTRP13 in myocardial I/R injury remains unclear. The aim of this study was to investigate the role of CTRP13 in H9c2 cells exposed to hypoxia/reoxygenation (H/R). Our results proved that CTRP13 protected H9c2 cells from H/R-stimulated oxidative stress and apoptosis via regulating the AMPK/Nrf2/ARE signaling pathway.

## Materials and Methods

### Myocardial I/R Injured Rat Model

The animal research protocol was approved by Institutional Animal Care and Use Committee of Kaifeng People's Hospital (Kaifeng, China) and conducted in accordance with the National Institutes of Health Guide for the Care and Use of Laboratory Animals. Myocardial I/R injury model was established according to the prior study<sup>10</sup> with some modifications. In brief, the rats (250-300 g) were anesthetized with pentobarbital sodium (50 mg/kg i.p.) before endotracheal intubation. After anesthesia, the animals were placed in a supine position and a lateral thoracotomy (1.5 cm incision between the third and fourth ribs) was performed to expose the left anterior descending coronary artery (LAD). A ligation using nylon suture was placed around the LAD at 3-5 mm for 45 min followed by 3 h of reperfusion. The rats were randomized into three groups ( $n = 5$  in each): sham group, subjected to the surgical procedures without occlusion of the LAD; I/R group, subjected to I/R and administration of NaCl 0.9% (1 ml/kg, intravenously); recombinant CTRP13 + I/R group, with identical procedures to the I/R group except for administration of recombinant CTRP13 protein (2 mg/kg, intravenously; TaKaRa Biotechnology Co., Ltd., Dalian, China) for 5 min before reperfusion.

### Measurement of Myocardial Infarction Size

To measure myocardial infarction size, hearts were excised and sectioned at 2 mm immediately. Then the heart slices were stained with 1% 2,3,5-triphenyltetrazolium (TTC) solution in PBS (pH 7.4) for 5 min at 37°C and then fixed in 10% formalin solution (pH 7.0) for 24 h. Images were taken with a Nikon camera and analyzed by using Image-ProPlus 6.0.

### Hematoxylin and Eosin (HE) Staining

Each heart was fixed in 4% paraformaldehyde-PBS for 30 min and cut into 5  $\mu$ m sections. Slides were then stained following the following steps: 70% ethyl alcohol (EtOH) for 10 s; diethylpyrocarbonate-treated water for 5 s; hematoxylin with RNAase inhibitor for 20 s; 70% EtOH for 30 s; eosin Y in 100% EtOH for 20 s and xylenes for 2 min. Finally, after being washed three times, the histological structure of myocardial tissues was observed with microscope (400 $\times$ ).

### Detection of Lactate Dehydrogenase (LDH) and Creatine kinase (CK) Levels

After the end of the reperfusion, plasma samples (1 mL) were obtained from myocardial tissues using a heparinized syringe and immediately centrifuged. The serum levels of LDH and CK were evaluated using commercial ELISA kits according to the manufacturer's instructions.

### Cell Culture

H9c2 cells from ATCC (Manassas, VA, USA) were cultured in Dulbecco's modified Eagle's medium (Hyclone, Logan, UT, USA) supplemented with 10% fetal bovine serum (FBS; Gibco, Rockville, MD, USA), 1% penicillin/streptomycin and maintained under 95% air/5% CO<sub>2</sub> at 37°C. To block the activation of AMPK, H9c2 cells were treated with 20  $\mu$ M of compound C (Sigma, St. Louis, MO, USA) for 24 h.

### Hypoxia/Reoxygenation (H/R) Model

H9c2 cells were maintained in glucose-free and serum-free DMEM and subjected to 8 h of hypoxia at 37°C in a controlled hypoxic plastic chamber (5% CO<sub>2</sub>/1% O<sub>2</sub>/94% N<sub>2</sub>). Following hypoxic exposure, H9c2 cells were subjected to 24 h of reoxygenation at 37°C in a normoxic incubator (95% air/5% CO<sub>2</sub>).

### SiRNA Transfection

The expression levels of CTRP13 and Nrf2 in H9c2 cells were suppressed by siRNA-mediated silencing through transfection with si-CTRP13 (GenePharma, Shanghai, China) and si-Nrf2 (GenePharma), respectively. H9c2 cells transfected with non-targeting control siRNA (si-NC; GenePharma) were used as controls. Lipofectamine RNAimax (Invitrogen, Carlsbad, CA, USA) was utilized for siRNA transfection following the manufacturer's instructions.

### CTRP13-Overexpressing Vector Transfection

CTRP13 overexpression was achieved in H9c2 cells by transfection with a CTRP13 full-length cDNA encoding plasmid pcDNA3.1-CTRP13. H9c2 cells transfected with pcDNA3.1 empty vector was used as controls. Lipofectamine 2000 (Invitrogen) was utilized for cell transfection according to the manufacturer's instructions.

### Cell Viability Assay

Cell viability was measured by MTT colorimetric assay. Briefly, H9c2 cells were plated in 96-well plates (10,000 cells per well in 100  $\mu$ l culture medium) and cultured for 24 h prior to H/R stimulation. Following different treatments, H9c2 cells were incubated for 1 h with 20  $\mu$ l of 0.5 mg/ml MTT solution, after which the medium was removed and replaced with 200  $\mu$ l DMSO to dissolve formazan crystals. Absorbance was measured at 490 nm using a microplate reader (Varioscan Flash, Thermo, Finland), and the absorbance values of control cells were set at 100%.

### Measurement of ROS

For in vivo assay, 10  $\mu$ m myocardium sections were washed three times by PBS for 5 min each time. Then, the sections were incubated ROS Fluorescent Probe-DHE (10  $\mu$ M, diluted by PBS) at 37°C for 30 min and then washed with PBS as before. Finally, the sections were observed with fluorescence microscopy.

Intracellular ROS was detected using a fluorescent dye, 2,7-dichlorodihydrofluorescein diacetate (DCDHF-DA). H9c2 cells were washed with PBS and then stained with 10  $\mu$ M H<sub>2</sub>-DCF-DA for 30 min at 37°C in the dark. The H9c2 cells were detected using a Microplate Fluorimeter (Bio-Tek Instruments, Winooski, VT, USA). The resulting fluorescence was recorded with an excitation wavelength of 490 nm and an emission wavelength of 525 nm.

### Detection of Superoxide Dismutase (SOD) and Catalase (CAT) Activity

The whole cell lysates of H9c2 cells were prepared using RIPA lysis buffer (Jiancheng Biochemical, Nanjing, China) according to manufacturer's instructions. Following the determination of proteins amount using the BCA assay (Jiancheng Biochemical), the activities of SOD and CAT were examined using commercial ELISA kits (Jiancheng Biochemical). Finally, the samples were measured using a Powerwave microplate spectrophotometer (Bio-Tek Instruments) at a wavelength of 450 nm.

### Detection of Caspase-3 Activity

Caspase-3 activity of H9c2 cells was measured with a Caspase-3 Colorimetric Assay Kit (Medical and Biological Laboratories, Nagoya, Japan) according to the manufacturer's protocols. Briefly, cell lysates of H9c2 cells were incubated at

37°C with caspase 3 substrates, Ac-DEVD-pNA and then the liberated p-NA was measured at 405 nm using a spectrophotometer (Molecular Devices, Sunnyvale, CA, USA).

### Terminal Deoxynucleotidyl Transferase dUTP Nick end Labeling (TUNEL) Assay

Cells were fixed with 4% paraformaldehyde and permeabilized by 0.5% Triton X-100. Then, cells were subjected to TUNEL staining (TdT Enzyme, TdT Buffer and TAM-dUTP Mixture) for 2 h at 37°C in the dark. Finally, the numbers of TUNEL-positive cells were observed and counted with a fluorescence microscope.

Cardiomyocyte apoptosis in heart tissue was also detected by TUNEL assay.

### ELISA

The level of CTRP13 in cell medium was evaluated using commercial CTRP13 ELISA kit according to the manufacturer's protocol.

### qRT-PCR Assay

Total RNA was isolated from H9c2 cells with a RNeasy mini kit (Qiagen, Hilden, Germany) as described in the manufacturer's manual. The obtained RNA was then used for the cDNA synthesis and qPCR experiments with Transcriptor First Strand cDNA synthesis Kit (Roche Diagnostics, Mannheim, Germany) and Faststart Essential DNA Green Master (Roche Diagnostics). The relative gene expression of CTRP13 normalized to the internal control gene  $\beta$ -actin was obtained by the  $2^{-\Delta\Delta C_t}$  method. The primers of CTRP13, forward, 5'-GACACGGAGCATTGTATGCAACAGG-3', and reverse, 5'-ACGGCTTCAGTGGTATTGTTCTGC A-3'. The primers of  $\beta$ -actin, forward, 5'-CGAGTACAACCTTCTTGACAGC-3', and reverse, 5'- ACCCATACCCACCATCACAC-3'.

### Western Blot

The cells were lysed in RIPA lysis buffer (Beyotime, Beijing, China) containing 1% protease and phosphatase inhibitor (Roche Diagnostics, Basel, Switzerland). Equal concentration of proteins (30  $\mu$ g/lane) in loading buffer was boiled at 100°C for 5 min and then separated on a 10% sodium dodecyl sulfate-polyacrylamide gel (SDS-PAGE) and transferred to a nitrocellulose membrane. The membranes were blocked for 1 h in 5% (wt/vol) nonfat dry milk (in TBST buffer: TBS buffer containing 0.05% Tween 20). Incubation with the primary antibody against CTRP13 (ab230660; Abcam, Cambridge, MA, USA), bax (#2772; Cell Signaling Technology, Boston, MA, USA), bcl-2 (ab59348; Abcam), LC3 (ab48394; Abcam); p-AMPK (#PA5-17831; Invitrogen), AMPK (#PA5-105297; Invitrogen), Nrf2 (ab137550; Abcam), lamin B2 (#PA5-85915; Invitrogen), or  $\beta$ -actin (ab8227; Abcam) was carried out overnight at 4°C. After three washes with TBST

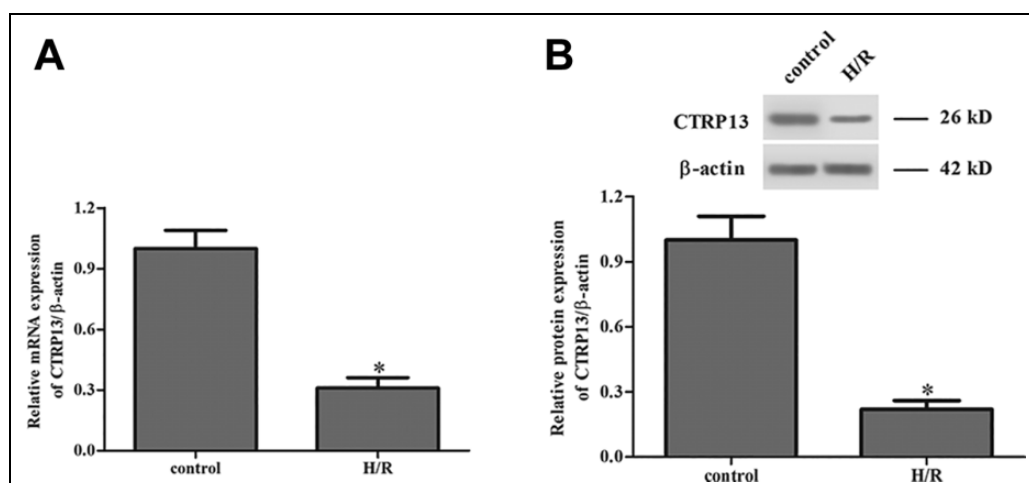


**Figure 1.** The expression levels of CTRP13 in H9c2 cells with or without H/R stimulation. The mRNA and protein levels of CTRP13 were detected using qRT-PCR and western blot, respectively. (A) Results from qRT-PCR. (B) Results from western blot.  $n = 4$ . \* $P < 0.05$  vs. control group.

buffer, the membranes were incubated with the appropriate horseradish peroxidase-linked anti-rabbit secondary antibody (#7074; Cell Signaling Technology), diluted 1:3000 in TBST buffer for 45 min at room temperature. Following three washes with TBST buffer, the bands were visualized using the enhanced chemiluminescence (ECL) detection system (Amersham Pharmacia, Piscataway, NJ, USA).

### Luciferase Reporter Assay

The ARE-driven luciferase reporter plasmid pGL6-ARE (4 ng) and Renilla luciferase pRL-TK vector (10 ng) were mixed together with OPTI-MEM and transfected into H9c2 cells. The luciferase activity was measured using a fluorescence microplate reader with the dual-luciferase assay kit (Promega, Madison, WI, USA) according to the supplier's recommendations.

### Statistical Analysis

The results were generated from three independent experiments and analyzed by GraphPad Prism version 6.0 (GraphPad Software, San Diego, CA, USA). The statistical differences between two groups were calculated by two-tailed Student's *t*-test. The statistical differences among multiple groups (more than two groups) were calculated by one way-ANOVA, followed by post hoc scheffe test. Data are presented as means  $\pm$  SD. Differences were considered to be statistically significant when  $P < 0.05$ .

## Results

### The Expression of CTRP13 Was Down-Regulated in H9c2 Cells Exposed to H/R

We first investigated the expression levels of CTRP13 in H9c2 cells with or without H/R stimulation. H9c2 cells exposed to H/

R exhibited down-regulated expression of CTRP13 at mRNA level (Fig. 1A). Meanwhile, the protein level of CTRP13 was also significantly decreased in H9c2 cells exposed to H/R (Fig. 1B). Furthermore, the data of ELISA assay indicated that CTRP13 concentration in cell medium was lower in the H/R group than the control group (Supplemental Fig. 1).

### Overexpression of CTRP13 Improved the Viability of H9c2 Cells Exposed to H/R

In order to assess the role of CTRP13, H9c2 cells were transfected with pcDNA3.1-CTR13 and the efficiency of transfection was evaluated using qRT-PCR and western blot. Significant increases of CTRP13 mRNA and protein levels were observed in H/R-exposed H9c2 cells post transfection with pcDNA3.1-CTR13 (Figs. 2A, B). In addition, pcDNA3.1-CTR13 also greatly up-regulated the protein expression level of CTRP13 in H9c2 cells (Supplemental Fig. 2). Moreover, the results of MTT assay demonstrated that H/R exposure significantly decreased the viability of H9c2 cells, which was markedly rescued by CTRP13 overexpression (Fig. 2C); recombinant CTRP13 protein also improved cell viability in H9c2 cells in response to H/R (Supplemental Fig. 3), suggesting that CTRP13 had an important role in cell viability.

### Overexpression of CTRP13 Inhibited H/R-Induced Oxidative Stress in H9c2 Cells

In addition, detection of ROS production and activities of SOD and CAT were conducted following a 48 h transfection to monitor changes in oxidative stress. The results in Fig. 3A showed that the increased level of ROS in H/R-induced H9c2 cells was suppressed by overexpression of CTRP13. Exposure of H9c2 cells to H/R resulted in significant inhibitions of SOD and CAT activities, whereas overexpression of

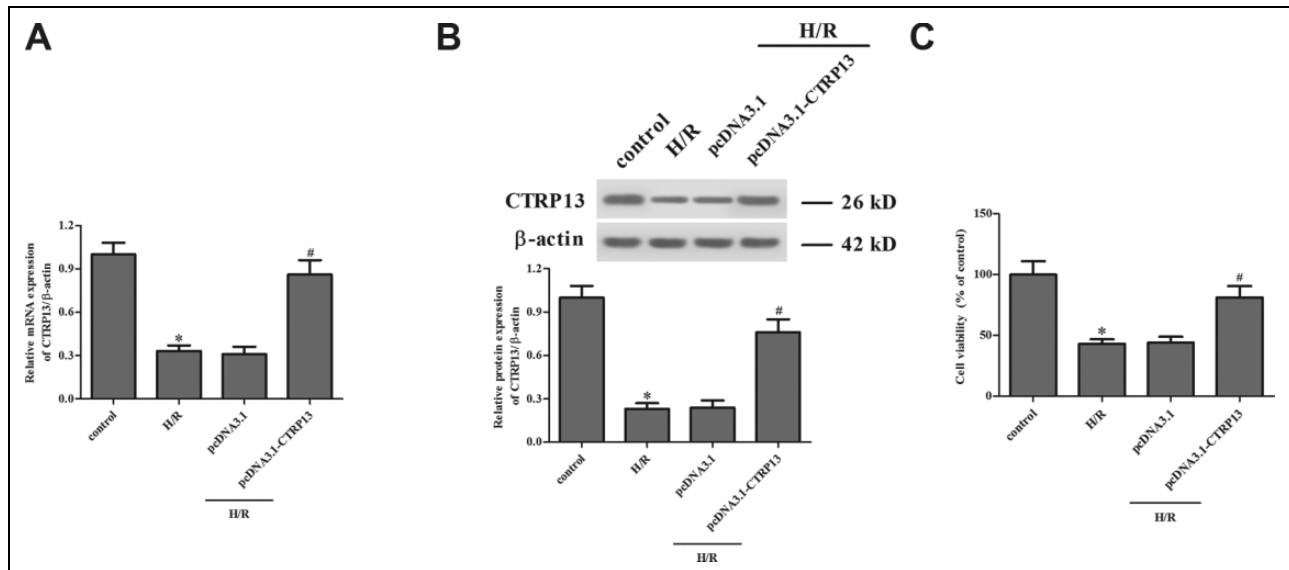


**Figure 2.** Overexpression of CTRP13 improved the viability of H9c2 cells exposed to H/R. H9c2 cells were transfected with pcDNA3.1-CTR13 or pcDNA3.1 for 48 h, then they were exposed to H/R injury. (A and B) The efficiency of transfection was evaluated using qRT-PCR and western blot. (C) Cell viability was measured by MTT assay.  $n = 4$ . \* $P < 0.05$  vs. control group; # $P < 0.05$  vs. H/R+pcDNA3.1 group.

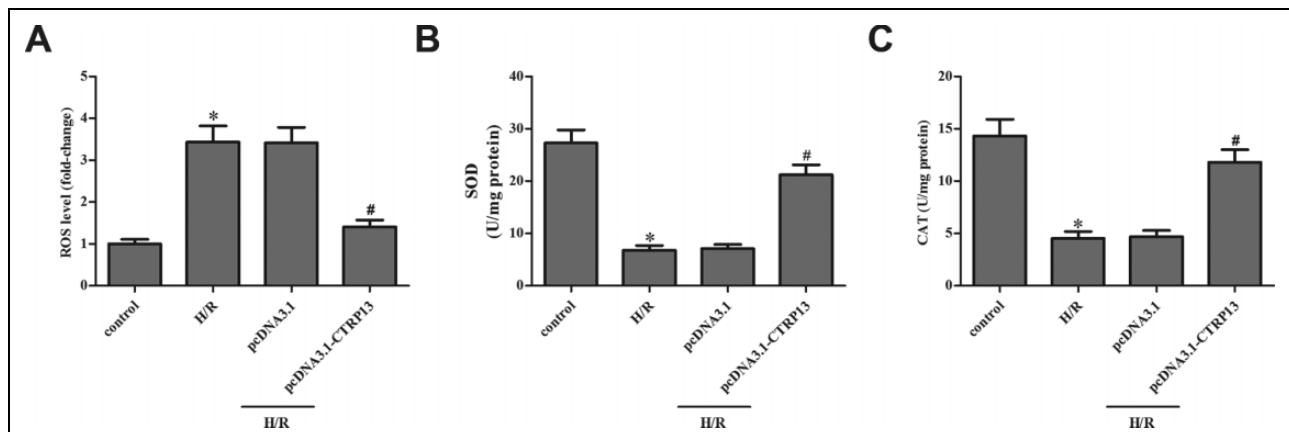


**Figure 3.** Overexpression of CTRP13 inhibited H/R-induced oxidative stress in H9c2 cells. H9c2 cells were transfected with pcDNA3.1-CTR13 or pcDNA3.1 for 48 h, then they were exposed to H/R injury. (A) ROS production in H9c2 cells. (B, C) Activities of SOD and CAT.  $n = 5$ . \* $P < 0.05$  vs. control group; # $P < 0.05$  vs. H/R+pcDNA3.1 group.

CTR13 led to increases in the activities of SOD and CAT (Figs. 3B, C). In addition, recombinant CTR13 protein also suppressed H/R-induced ROS level in H9c2 cells (Supplemental Fig. 3B).

### Overexpression of CTR13 Inhibited Apoptosis in H9c2 Cells After H/R Stimulation

Next, we performed the comparison of cell apoptosis between H9c2 cells treated with or without H/R. The results revealed that the caspase-3 activity was higher in H/R-induced H9c2 cells than in control H9c2 cells. However, the increased caspase-3 activity was reduced by

overexpression of CTR13 or recombinant CTR13 protein (Fig. 4A and Supplemental Fig. 3C). In addition, the protein expressions of bax and bcl-2 were assessed using western blot. As shown in Fig. 4B–D, the bax expression was increased, while bcl-2 expression was decreased in H9c2 cells after H/R treatment. These changes in the expressions of bax and bcl-2 were blocked by CTR13. Furthermore, TUNEL apoptosis assay revealed that the elevated apoptotic H9c2 cells induced by H/R stimulation was markedly decreased by CTR13 overexpression (Fig. 4E, F). We also found that CTR13 has no effect on the expression level of LC3-II in H9c2 cells in response to H/R (Supplemental Fig. 4).

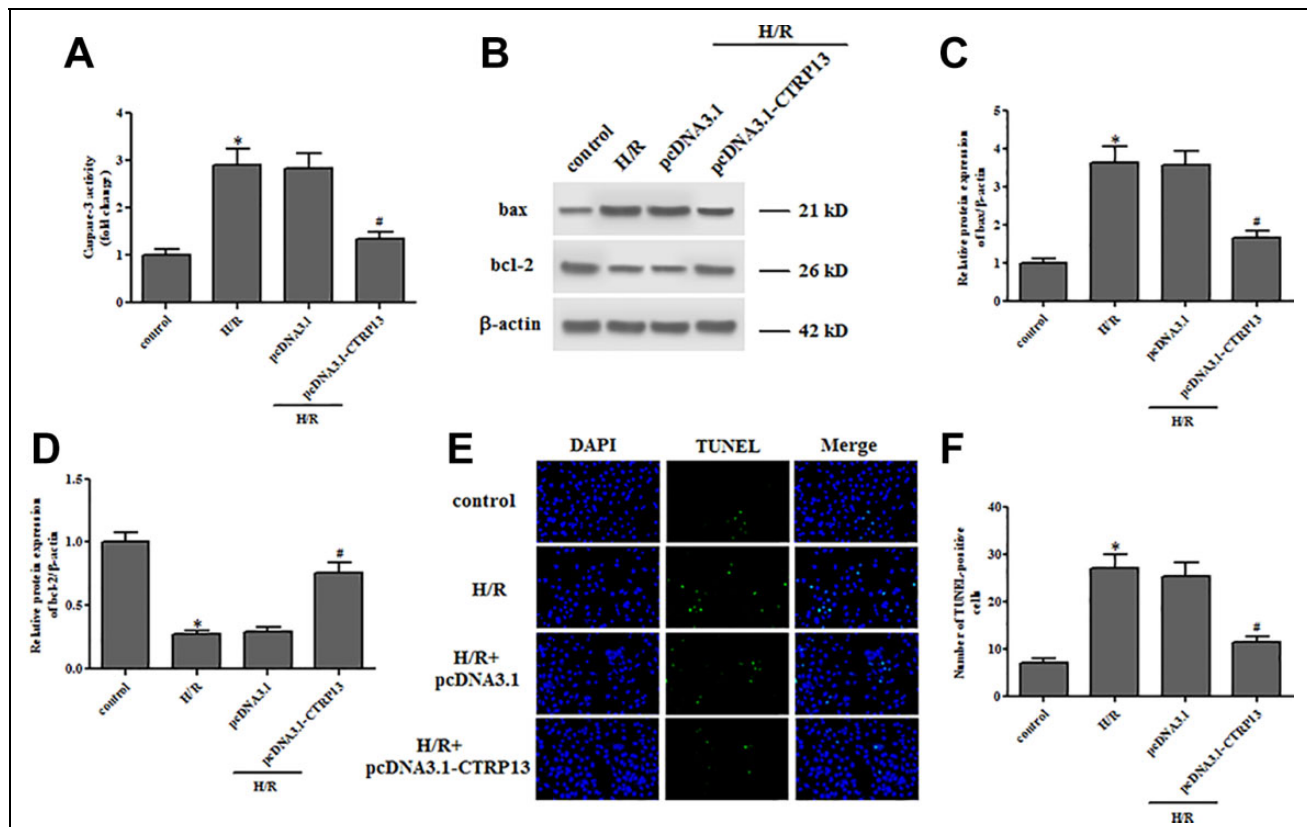


**Figure 4.** Overexpression of CTRP13 inhibited apoptosis in H9c2 cells after H/R stimulation. H9c2 cells were transfected with pcDNA3.1-CTR13 or pcDNA3.1 for 48 h, then they were exposed to H/R injury. (A) Caspase-3 activity in H9c2 cells. (B) Expression levels of bax and bcl-2 were measured by western blot. (C and D) Quantification analysis of bax and bcl-2. (E, F) The effect of CTRP13 overexpression on cell apoptosis was evaluated by TUNEL assay.  $n = 3$ . \* $P < 0.05$  vs. control group; # $P < 0.05$  vs. H/R+pcDNA3.1 group.

### Knockdown of CTRP13 Promoted H/R-Induced Oxidative Stress and Apoptosis in H9c2 Cells after H/R Stimulation

Subsequently, the expression of CTRP13 at both protein and mRNA levels was diminished in H9c2 cells through siRNA-mediated transient transfection, which was confirmed by western blot and qRT-PCR assays (Figs. 5A–C). Furthermore, we found that CTRP13 knockdown significantly decreased the viability and exacerbated the ROS generation in H/R exposed H9c2 cells (Fig. 5D, E). Moreover, the H/R-cause a significant increase in caspase-3 activity was promoted by knockdown of CTRP13 (Fig. 5F).

### Overexpression of CTRP13 Enhanced the Activation of AMPK/Nrf2/ARE Signaling Pathway in H/R-Stimulated H9c2 Cells

AMPK/Nrf2/ARE signaling pathway has been identified as an antioxidant signaling that is activated by ROS. We next evaluated the effect of CTRP13 on the activation of AMPK/Nrf2/ARE in H/R exposed H9c2 cells. Western blot

demonstrated that H/R stimulation increased the levels of p-AMPK and nuclear Nrf2, which were enhanced by CTRP13 (Fig. 6A–C). In addition, we also performed a luciferase reporter assay to explore the Nrf2 transcriptional activity. As indicated in Fig. 6D, the increased Nrf2 transcriptional activity was significantly enhanced by CTRP13 overexpression.

### CTR13 Regulates Nrf2/ARE Signaling Pathway Through AMPK in H9c2 Cells

To confirm the role of AMPK/Nrf2/ARE, compound C, an inhibitor of AMPK, was used to block the AMPK signaling. Treatment with compound C caused expected decrease in the expression level of nuclear Nrf2 in H9c2 cells (Fig. 7A, B). The luciferase reporter assay revealed that the CTRP13-induced an increase in Nrf2 transcriptional activity was reduced by compound C (Fig. 7C). Moreover, the regulatory effects of CTRP13 on cell viability, ROS level and caspase 3 activity were significantly reversed by AMPK inhibition (Fig. 7D–F). These results indicated that the regulation of CTRP13 on Nrf2/ARE signaling was mediated by AMPK in H9c2 cells.

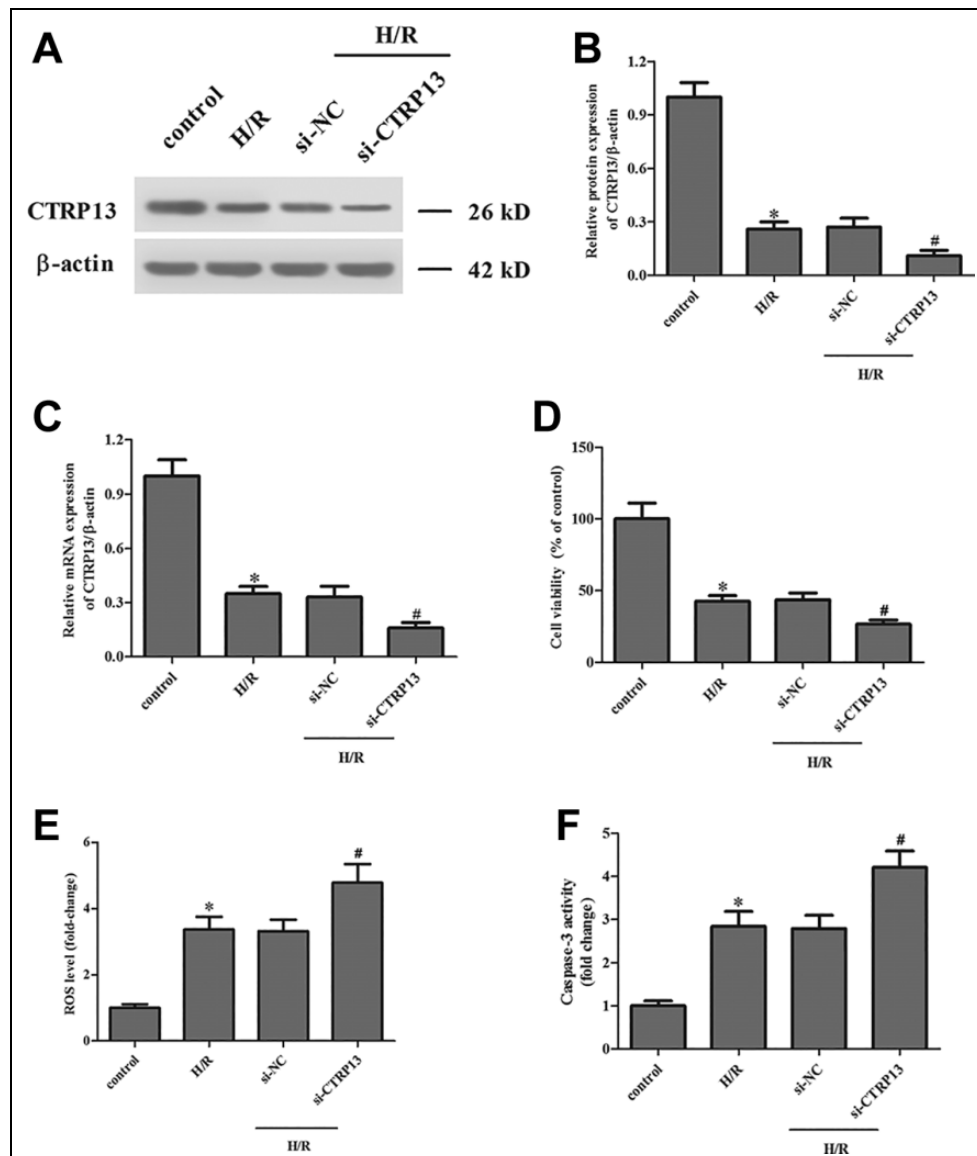


**Figure 5.** Knockdown of CTRP13 promoted H/R-induced oxidative stress and apoptosis in H9c2 cells after H/R stimulation. H9c2 cells were transfected with si-CTR13 or si-NC for 48 h, then they were exposed to H/R injury. (A–C) The efficiency of transfection was evaluated using western blot and qRT-PCR assays. (D) Cell viability was measured by MTT assay. (E) ROS production in H9c2 cells. (F) Caspase-3 activity in H9c2 cells.  $n = 4$ . \* $P < 0.05$  vs. control group; # $P < 0.05$  vs. H/R+si-NC group.

### Silencing of Nrf2 Reversed the Protective Effects of CTRP13 on H/R-Stimulated H9c2 Cells

Finally, H9c2 cells were transfected with si-Nrf2 to knockdown the Nrf2 expression and thereby explore the role of Nrf2 signaling. Results from western blot proved that knockdown of Nrf2 significantly decreased the nuclear expression of Nrf2 in H9c2 cells transfected with pcDNA3.1-CTR13 following H/R exposure (Fig. 8A, B). The luciferase reporter assay revealed that silencing of Nrf2 significantly attenuated the promotion effect of CTRP13 on Nrf2/ARE-mediated transcription activity (Fig. 8C). Furthermore, we found that silencing of Nrf2 reversed the effects of CTRP13 on cell

viability, ROS level and caspase 3 activity in H/R-stimulated H9c2 cells (Fig. 8D–F).

### Recombinant CTRP13 Protein Attenuated Myocardial I/R-Induced Injury in Rats

Finally, we examined the role of CTRP13 in myocardial I/R-induced injury in rats. The transduction efficiency of CTRP13 was shown in Fig. 9A. As indicated in Fig. 9B, C, recombinant CTRP13 protein significantly reduced myocardial infarct size compared with that in the I/R group. In addition, we found that recombinant CTRP13 protein greatly inhibited apoptosis and ROS level in the

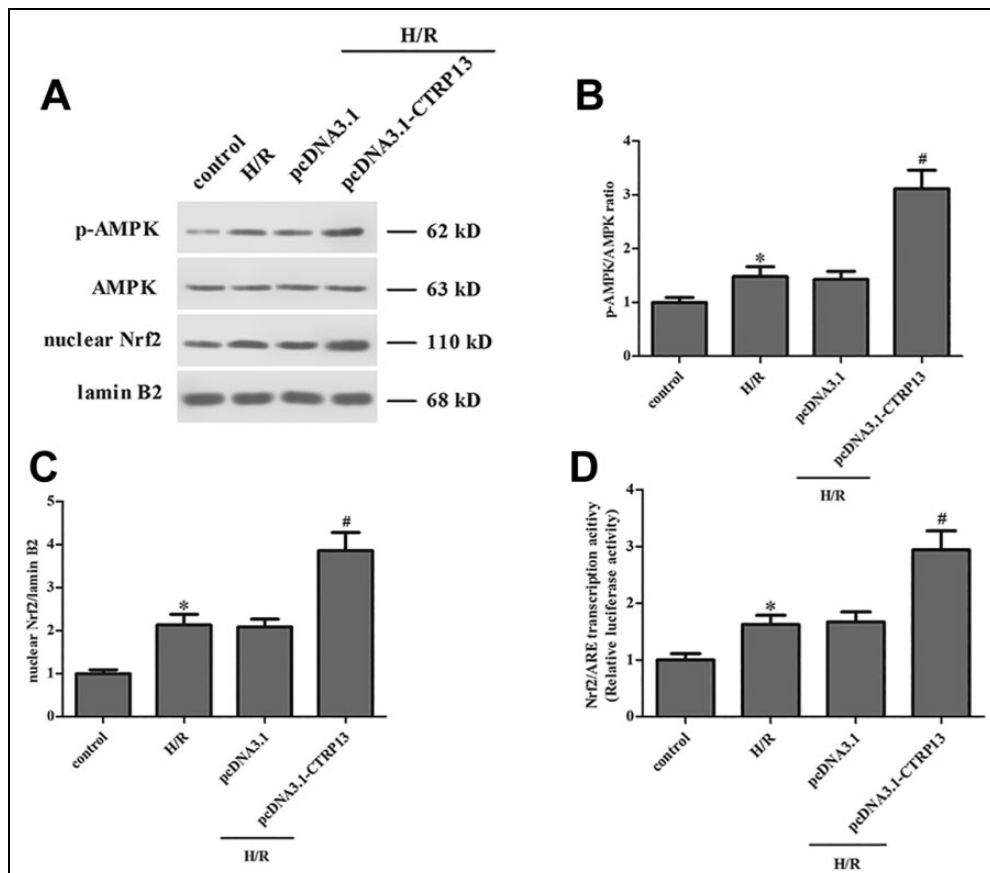


**Figure 6.** Overexpression of CTRP13 enhanced the activation of AMPK/Nrf2/ARE signaling pathway in H/R-stimulated H9c2 cells. (A–C) Western blot was performed to detect the expression levels of AMPK, p-AMPK and nuclear Nrf2. (D) Luciferase reporter assay was conducted to explore the Nrf2 transcriptional activity.  $n = 3$ . \* $P < 0.05$  vs. control group; # $P < 0.05$  vs. H/R+pcDNA3.1 group.

myocardium following I/R rats (Fig. 9D, E). Furthermore, the serum levels of LDH and CK were significantly increased at the end of reperfusion in the I/R group, while these effects were suppressed by recombinant CTRP13 protein (Fig. 9F, G).

### Recombinant CTRP13 Protein Enhanced the Activation of AMPK/Nrf2 Signaling Pathway in Myocardial I/R Rats

We also investigated the effect of recombinant CTRP13 on AMPK/Nrf2 pathway in myocardial I/R rats. The results indicated that recombinant CTRP13 protein significantly enhanced I/R-induced the levels of p-AMPK and nuclear Nrf2 in the myocardium following I/R rats (Fig. 10A–C).

## Discussion

ROS comprise free radicals such as superoxide, hydroxyl radical, and singlet oxygen, as well as non-radical species such as hydrogen peroxide<sup>11</sup>. ROS are byproducts generated through a variety of extracellular and intracellular

actions and have drawn attention as novel signal mediators in I/R injury<sup>12,13</sup>. The rapid restoration of blood flow increases the level of tissue oxygenation and accounts for a second burst of ROS generation, which leads to tissues reperfusion injury via inducing oxidative stress and apoptosis<sup>14</sup>. CTRP13 has been found to reduce ROS overproduction and improve nitric oxide (NO) production and endothelial NO synthase (eNOS) coupling in the aortae of diabetic mice<sup>15</sup>. Taken together with the function of CTRP13 in cardiovascular diseases, we aimed to evaluate the role of CTRP13 in myocardial I/R injury in the present study. We found that the expression of CTRP13 was down-regulated in H9c2 cells exposed to H/R, implying the potential involvement of CTRP13. Further gain-and lose-of function assays proved that CTRP13 attenuated H/R-induced ROS overproduction and reduction in SOD and CAT activities. The H/R-induced cell apoptosis of H9c2 cells was also prevented by CTRP13. The results indicated that CTRP13 protected the H9c2 cells from H/R-induced cell injury.

It has been demonstrated that ROS plays central roles in determination of cell fate as second messengers and has impacts on several signaling pathways including NF- $\kappa$ B,



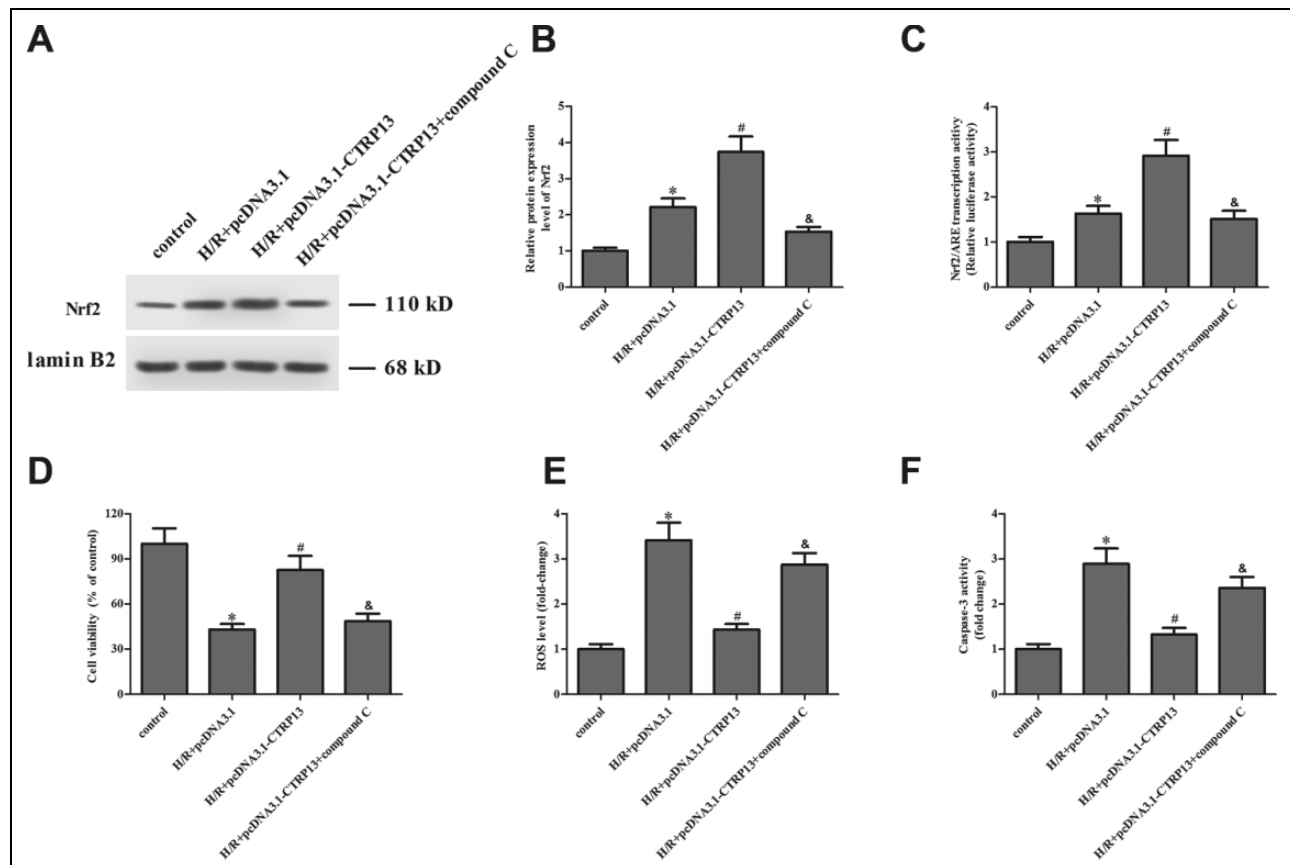


**Figure 7.** Effect of AMPK inhibition on CTRP13-mediated activation of Nrf2/ARE signaling pathway in H/R-induced H9c2 cells. H9c2 cells were transfected with pcDNA3.1-CTR13 for 48 h in the presence of Compound C (10  $\mu$ M), and then they were subjected to H/R injury. (A) Nrf2 nuclear protein expression was measured by western blot. (B) Quantification analysis of Nrf2. (C) Luciferase reporter assay was conducted to explore the Nrf2 transcriptional activity. (D) Cell viability in H9c2 cells. (E) ROS production in H9c2 cells. (F) Caspase-3 activity in H9c2 cells.  $n = 4$ . \* $P < 0.05$  vs. control group; # $P < 0.05$  vs. H/R+pcDNA3.1 group; & $P < 0.05$  vs. H/R+pcDNA3.1-CTR13 group.

MAPKs, AMPK, Keap1-Nrf2-ARE, and PI3K-Akt<sup>16</sup>. Hence, reducing the ROS production and regulating related pathways may be the novel therapeutic strategy to reduce the tissue damage related to both ischemia and reperfusion. AMPK is a crucial energy sensor in cells, which plays an important role in the regulation of cellular energy homeostasis and metabolic pathways<sup>17,18</sup>. There is evidence that AMPK can be activated in response to ROS signaling under metabolic stress, including inflammation and oxidative stress<sup>19</sup>. Considering the properties of AMPK, many researchers have demonstrated that AMPK is involved in the myocardial I/R injury. Exosomes derived from mesenchymal stem cells rescue myocardial I/R injury via AMPK and Akt pathways<sup>20</sup>. Trimetazidine exerts its protective effect on myocardial I/R injury through activating AMPK and ERK signaling pathway<sup>21</sup>. Barbaloin pretreatment attenuates myocardial I/R injury by improving hemodynamic function and limiting infarction size via activation of AMPK<sup>22</sup>. These findings indicate that AMPK may be a therapeutic target for the treatment of myocardial I/R injury. Our results showed that overexpression of CTRP13 enhanced the activation of AMPK in H/R-stimulated H9c2

cells, as evidenced by increased expression levels of p-AMPK. In consistent with our findings, previous study has demonstrated that CTRP13 promotes glucose uptake in adipocytes, myotubes, and hepatocytes via activation of the AMPK signaling pathway<sup>23</sup>. CTRP13 exhibits protective role in hepatic sinusoidal capillarization induced by high glucose via activating CAMKK $\beta$ /AMPK pathway<sup>24</sup>.

It has recently been reported that AMPK functions through interaction with various signaling pathways<sup>25</sup>. Among the several AMPK-related signaling pathways, the Nrf2 signaling pathway plays a significant role in the regulation of genes and proteins with cyto-protective functions<sup>26</sup>. To date, abundant reports have revealed that Nrf2 signaling pathway presents a prominent role in protecting myocardial I/R injury and serves as a therapeutic target. Down-regulation of miR-320 exerts protective effects on myocardial I/R injury by facilitating Nrf2 expression<sup>27</sup>. Epidermal growth factor (EGF) decreases oxidative stress and protects against myocardial I/R injury through activating Nrf2 signaling pathway<sup>28</sup>. The novel curcumin analogue 14p acts as a promising antioxidant to decrease oxidative stress and limit myocardial I/R injury via

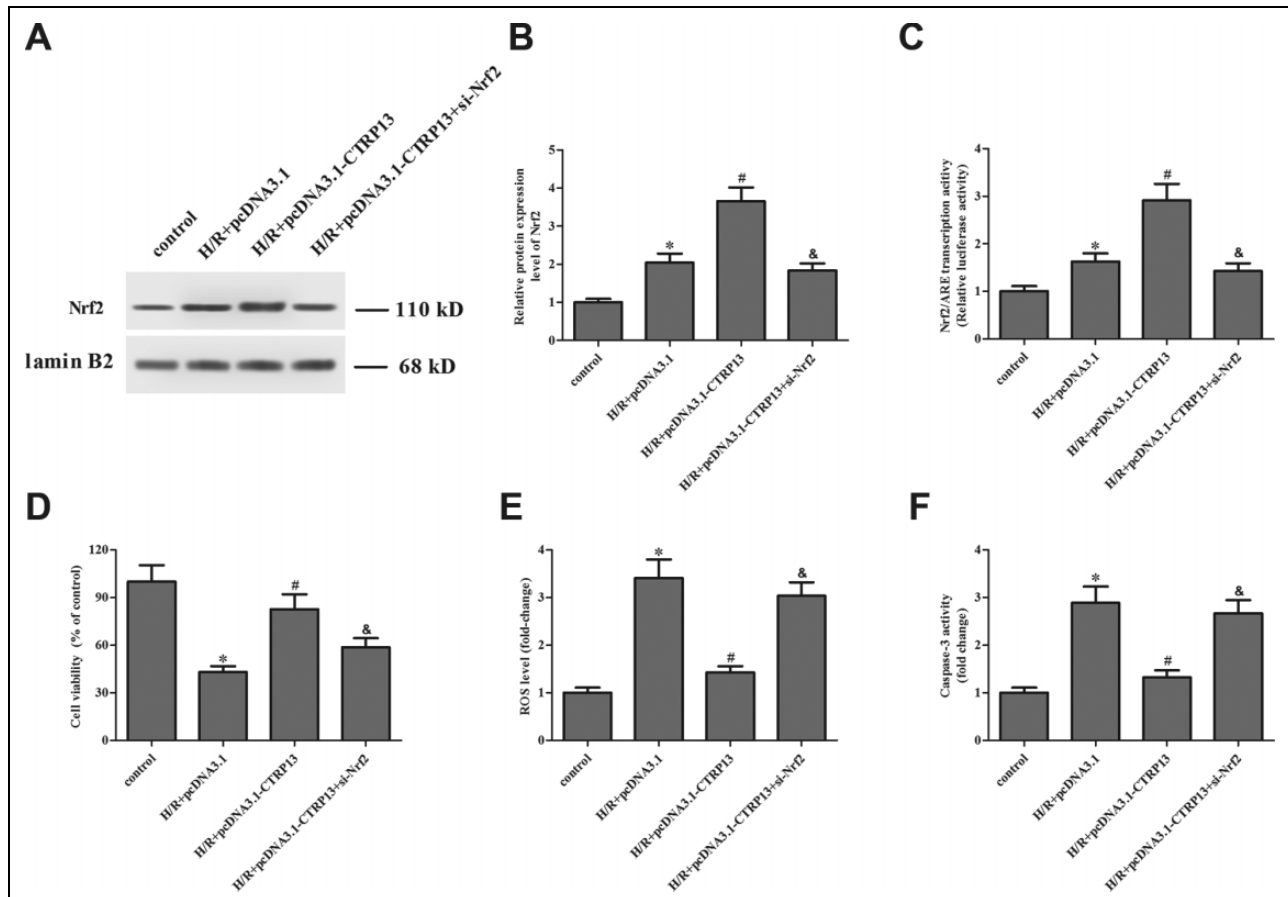


**Figure 8.** Silencing of Nrf2 reversed the protective effects of CTRP13 on H/R-stimulated H9c2 cells. H9c2 cells were co-transfected with pcDNA3.1-CTR13 and si-Nrf2 for 48 h, then subjected to H/R injury. (A) Nrf2 nuclear protein expression was measured by western blot. (B) Quantification analysis of Nrf2. (C) Nrf2/ARE-mediated transcription activity was assessed by luciferase reporter assay. (D) Cell viability in H9c2 cells. (E) ROS production in H9c2 cells. (F) Caspase-3 activity in H9c2 cells.  $n = 3$ . \* $P < 0.05$  vs. control group; # $P < 0.05$  vs. H/R+pcDNA3.1 group; & $P < 0.05$  vs. H/R+pcDNA3.1-CTR13 group.

activating Nrf2<sup>29</sup>. In this study, we found that the increased expression level of nuclear Nrf2 in H/R-stimulated H9c2 cells was enhanced by CTRP13. Since Nrf2 is a transcription factor that exerts its function through binding to the ARE<sup>30</sup>, we also investigated the effect of CTRP13 on Nrf2 transcriptional activity. We observed that CTRP13 also elevated the Nrf2 transcriptional activity in H/R-stimulated H9c2 cells, implying that CTRP13 induced the activation of Nrf2/ARE antioxidant signaling.

There is an emerging relationship between the two major regulators of the antioxidant response, AMPK and Nrf2, in the progression of myocardial I/R injury. Galanthamine improves myocardial I/R-induced cardiac dysfunction, endoplasmic reticulum stress-related apoptosis, and myocardial fibrosis by activating AMPK/Nrf2 pathway in rats<sup>31</sup>. Mulberry granules (MLD) protects against diabetic-associated cardiomyopathy by suppressing oxidative stress induced by hyperglycemia and myocardial I/R through the AMPK/Nrf2 signaling pathway<sup>32</sup>. Therefore, the development of novel therapeutics with a dual AMPK and Nrf2 activation profile may have important value. We next used

compound C, an inhibitor of AMPK, to block the AMPK signaling. The results showed that treatment with compound C suppressed the activation of Nrf2/ARE antioxidant signaling. Moreover, silencing of Nrf2 reversed the protective effects of CTRP13 on H/R-stimulated H9c2 cells. Taken together, these results suggested that CTRP13 exerted its roles via regulating the AMPK/Nrf2/ARE signaling pathway. CaMKK $\beta$ , as one of the upstream kinase of AMPK, formed a stable complex with AMPK and promoted AMPK activation. Zhang et al. reported that CTRP13 protects against high glucose-induced hepatic sinusoidal capillarization by activating CaMKK $\beta$ /AMPK pathway<sup>24</sup>. However, how did CTRP13 regulate AMPK signaling pathway in this study will require further studies.

In summary, our study first revealed that CTRP13 exerted protective roles in H/R-stimulated H9c2 cells through inhibition of oxidative stress and apoptosis. The protective effects of CTRP13 were mediated by regulating the AMPK/Nrf2/ARE signaling pathway. Therefore, CTRP13 may be a novel therapeutic target in the treatment of myocardial I/R injury.

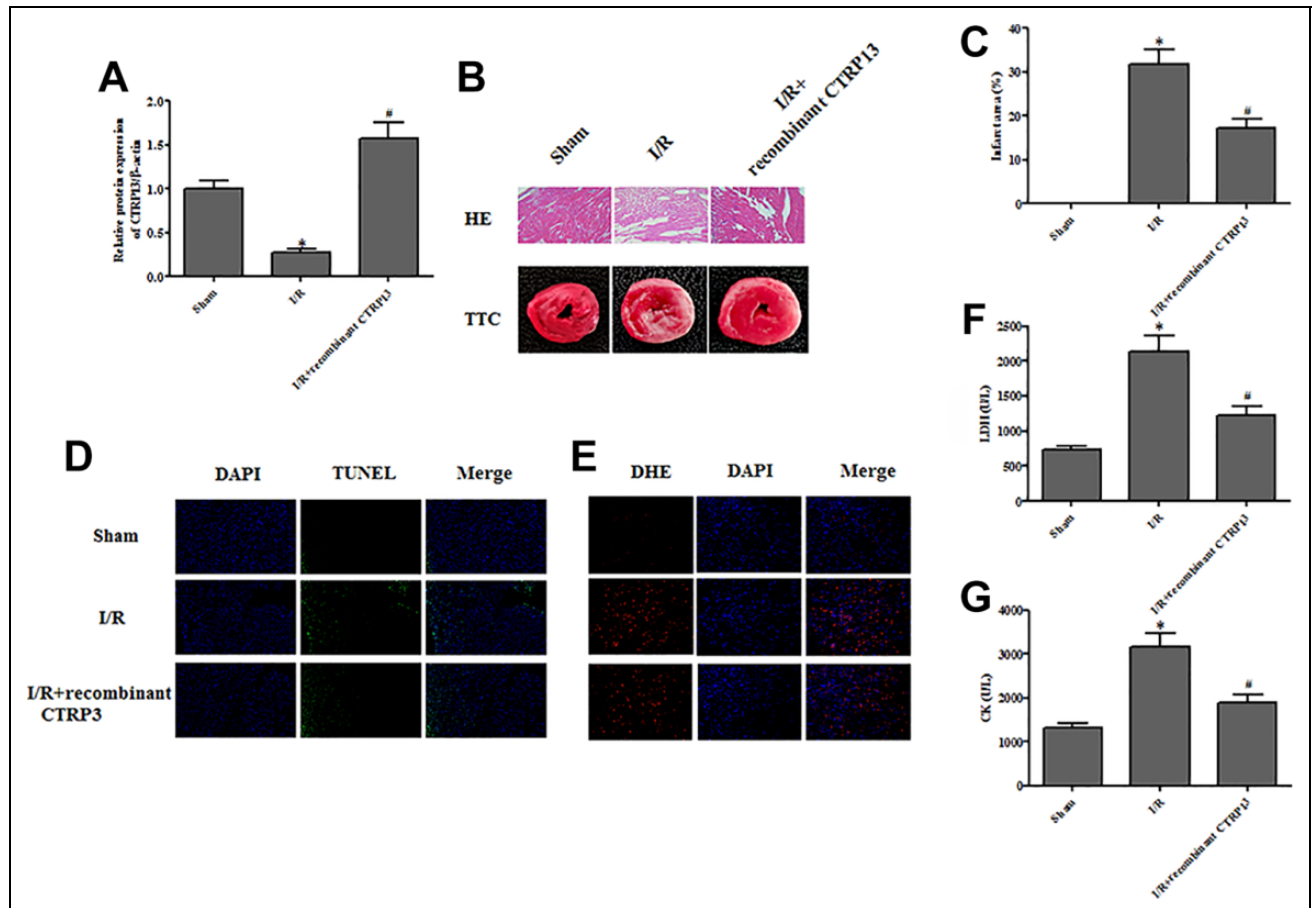


**Figure 9.** Recombinant CTRP13 protein attenuated myocardial I/R-induced injury in rats. (A) The transduction efficiency of CTRP13 in the I/R rats. (B, C) Illustration of HE staining and TTC staining of the myocardial tissues in different rat groups. (C) Myocardial infarct size was determined. (D) Representative photomicrographs ( $\times 200$ ) of TUNEL staining in myocardial I/R tissue. Green fluorescence indicates TUNEL-positive apoptotic nuclei; blue fluorescence indicates total cardiomyocyte nuclei. (E) ROS were stained with DHE (red) and nuclei with DAPI (blue). (F, G) The serum levels of LDH and CK were evaluated using commercial ELISA kits.  $n = 5$ . \* $P < 0.05$  vs. Sham group; # $P < 0.05$  vs. I/R group.

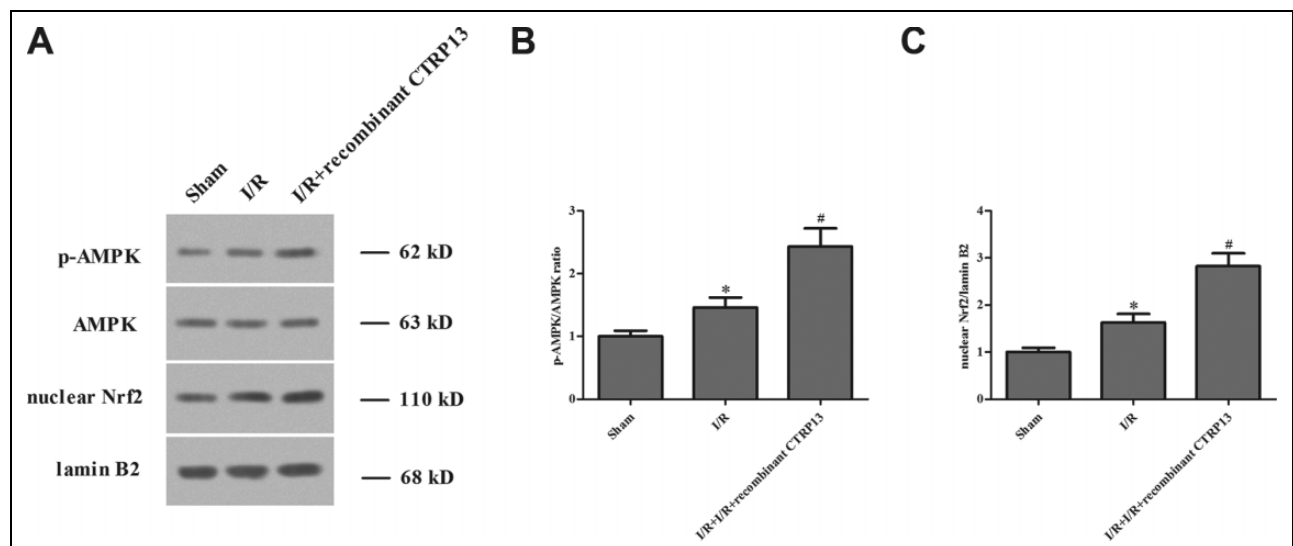


**Figure 10.** Recombinant CTRP13 protein enhanced the activation of AMPK/Nrf2 signaling pathway in myocardial I/R rats. (A–C) Western blot was performed to detect the expression levels of AMPK, p-AMPK and nuclear Nrf2 in the myocardium following I/R rats.  $n = 4$ . \* $P < 0.05$  vs. Sham group; # $P < 0.05$  vs. I/R group.

## Ethical Approval

This study was approved by the Ethics Committee at the Kaifeng People's Hospital (Kaifeng, China).

## Statement of Human and Animal Rights

All procedures in this study were conducted in accordance with Kaifeng People's Hospital OF ETHICS COMMITTEE'S OR INSTITUTIONAL REVIEW BOARD'S (APPROVAL NUMBER: 00507) approved protocols.

## Statement of Informed Consent

Written informed consent was obtained from the patients for their anonymized information to be published in this article.


## Declaration of Conflicting Interests

The author(s) declared no potential conflicts of interest with respect to the research, authorship, and/or publication of this article.

## Funding

The author(s) received no financial support for the research, authorship, and/or publication of this article.

## ORCID iD

Weifeng Jiang  <https://orcid.org/0000-0002-9626-8831>

## Supplemental Material

Supplemental material for this article is available online.

## References

- Lu L, Liu M, Sun R, Zheng Y, Zhang P. Myocardial infarction: symptoms and treatments. *Cell Biochem Biophys*. 2015;72(3):865–867.
- Saleh M, Ambrose JA. Understanding myocardial infarction. *F1000Res*. 2018;7:F1000 Faculty Rev-1378.
- Pollard TJ. The acute myocardial infarction. *Prim Care*. 2000;27(3):631–649;vi.
- Rentrop KP, Feit F. Reperfusion therapy for acute myocardial infarction: concepts and controversies from inception to acceptance. *Am Heart J*. 2015;170(5):971–980.
- Cadenas S. ROS and redox signaling in myocardial ischemia-reperfusion injury and cardioprotection. *Free Radic Biol Med*. 2018;117:76–89.
- Schaffler A, Buechler C. CTRP family: linking immunity to metabolism. *Trends Endocrinol Metab*. 2012;23(4):194–204.
- Seldin MM, Tan SY, Wong GW. Metabolic function of the CTRP family of hormones. *Rev Endocr Metab Disord*. 2014;15(2):111–123.
- Si Y, Fan W, Sun L. A review of the relationship between ctrp family and coronary artery disease. *Curr Atheroscler Rep*. 2020;22(6):22.
- Wang C, Xu W, Liang M, Huang D, Huang K. CTRP13 inhibits atherosclerosis via autophagy-lysosome-dependent degradation of CD36. *FASEB J*. 2019;33(2):2290–2300.
- Pfeffer MA, Pfeffer JM, Fishbein MC, Fletcher PJ, Spadaro J, Kloner RA, Braunwald E. Myocardial infarct size and ventricular function in rats. *Circ Res*. 1979;44(4):503–512.
- Brieger K, Schiavone S, Miller FJ Jr., Krause KH. Reactive oxygen species: from health to disease. *Swiss Med Wkly*. 2012;142:w13659.
- Minutoli L, Puzzolo D, Rinaldi M, Irrera N, Marini H, Arcoraci V, Bitto A, Crea G, Pisani A, Squadrito F, Trichilo V, et al. ROS-Mediated NLRP3 inflammasome activation in brain, heart, kidney, and testis ischemia/reperfusion injury. *Oxid Med Cell Longev*. 2016;2016:2183026.
- Zhou T, Chuang CC, Zuo L. Molecular characterization of reactive oxygen species in myocardial ischemia-reperfusion injury. *Biomed Res Int*. 2015;2015:864946.
- Rodrigo R, Fernandez-Gajardo R, Gutierrez R, Matamala JM, Carrasco R, Miranda-Merchak A, Feuerhake W. Oxidative stress and pathophysiology of ischemic stroke: novel therapeutic opportunities. *CNS Neurol Disord Drug Targets*. 2013;12(5):698–714.
- Wang C, Chao Y, Xu W, Liang M, Deng S, Zhang D, Huang K. CTRP13 preserves endothelial function by targeting GTP cyclohydrolase 1 in diabetes. *Diabetes*. 2020;69(1):99–111.
- Zhang J, Wang X, Vikash V, Ye Q, Wu D, Liu Y, Dong W. ROS and ROS-mediated cellular signaling. *Oxid Med Cell Longev*. 2016;2016:4350965.
- Hardie DG, Ross FA, Hawley SA. AMPK: a nutrient and energy sensor that maintains energy homeostasis. *Nat Rev Mol Cell Biol*. 2012;13(4):251–262.
- Garcia D, Shaw RJ. AMPK: mechanisms of cellular energy sensing and restoration of metabolic balance. *Mol Cell*. 2017;66(6):789–800.
- Zhao Y, Hu X, Liu Y, Dong S, Wen Z, He W, Zhang S, Huang Q, Shi M. ROS signaling under metabolic stress: cross-talk between AMPK and AKT pathway. *Mol Cancer*. 2017;16(1):79–90.
- Liu L, Jin X, Hu CF, Li R, Zhou Z, Shen CX. Exosomes derived from mesenchymal stem cells rescue myocardial ischaemia/reperfusion injury by inducing cardiomyocyte autophagy via AMPK and Akt pathways. *Cell Physiol Biochem*. 2017;43(1):52–68.
- Liu Z, Chen JM, Huang H, Kuznicki M, Zheng S, Sun W, Quan N, Wang L, Yang H, Guo HM, Li J, et al. The protective effect of trimetazidine on myocardial ischemia/reperfusion injury through activating AMPK and ERK signaling pathway. *Metabolism*. 2016;65(3):122–130.
- Zhang P, Liu X, Huang G, Bai C, Zhang Z, Li H. Barbaloin pretreatment attenuates myocardial ischemia-reperfusion injury via activation of AMPK. *Biochem Biophys Res Commun*. 2017;490(4):1215–1220.
- Wei Z, Peterson JM, Wong GW. Metabolic regulation by C1q/TNF-related protein-13 (CTRP13): activation OF AMP-activated protein kinase and suppression of fatty acid-induced JNK signaling. *J Biol Chem*. 2011;286(18):15652–15665.
- Zhang Q, Niu X, Tian L, Liu J, Niu R, Quan J, Yu J, Lin W, Qian Z, Zeng P. CTRP13 attenuates the expression of LN and CAV-1 Induced by high glucose via CaMKKbeta/AMPK pathway in rLSECs. *Aging (Albany NY)*. 2020;12(12):11485–11499.

25. Cao W, Li J, Hao Q, Vadgama JV, Wu Y. AMP-activated protein kinase: a potential therapeutic target for triple-negative breast cancer. *Breast Cancer Res.* 2019;21(1):29.
26. Bellezza I, Giambanco I, Minelli A, Donato R. Nrf2-Keap1 signaling in oxidative and reductive stress. *Biochim Biophys Acta Mol Cell Res.* 2018;1865(5):721–733.
27. Zhu XA, Gao LF, Zhang ZG, Xiang DK. Down-regulation of miR-320 exerts protective effects on myocardial I-R injury via facilitating Nrf2 expression. *Eur Rev Med Pharmacol Sci.* 2019;23(4):1730–1741.
28. Ma J, Jin G. Epidermal growth factor protects against myocardial ischaemia reperfusion injury through activating Nrf2 signalling pathway. *Free Radic Res.* 2019;53(3):313–323.
29. Li W, Wu M, Tang L, Pan Y, Liu Z, Zeng C, Wang J, Wei T, Liang G. Novel curcumin analogue 14p protects against myocardial ischemia reperfusion injury through Nrf2-activating anti-oxidative activity. *Toxicol Appl Pharmacol.* 2015;282(2):175–183.
30. Tonelli C, Chio IIC, Tuveson DA. Transcriptional regulation by Nrf2. *Antioxid Redox Signal.* 2018;29(17):1727–1745.
31. Hou X, Fu M, Cheng B, Kang Y, Xie D. Galanthamine improves myocardial ischemia-reperfusion-induced cardiac dysfunction, endoplasmic reticulum stress-related apoptosis, and myocardial fibrosis by suppressing AMPK/Nrf2 pathway in rats. *Ann Transl Med.* 2019; 7(22):634–643.
32. Liu Y, Zhao YB, Wang SW, Zhou Y, Tang ZS, Li F. Mulberry granules protect against diabetic cardiomyopathy through the AMPK/Nrf2 pathway. *Int J Mol Med.* 2017; 40(3):913–921.